



# Soil geochemistry as a tool for the origin investigation and environmental evaluation of urban parks in Mashhad city, NE of Iran

Seyed Ali Mazhari<sup>1</sup> · Ali Reza Mazloumi Bajestani<sup>1</sup> · Fereshteh Hatefi<sup>1</sup> · Kazem Aliabadi<sup>2</sup> · Faezeh Haghighi<sup>3</sup>

Received: 11 January 2018 / Accepted: 26 June 2018 / Published online: 2 July 2018  
© Springer-Verlag GmbH Germany, part of Springer Nature 2018

## Abstract

The total concentration of major oxides and trace elements, sequential extraction of heavy metals, and Pb isotope signatures of park soils were investigated in Mashhad, the largest city in northeastern Iran. The geochemical characteristics of park soils show two different trends: high silica soils (HSS) and low silica soils (LSS). The elements such as Mg, Fe, As, Co, Cr, Cu, Mn, Ni, Pb, Sn, and Zn were concentrated in LSS, while HSS samples were enriched of Si, Ga, Li, Nb, Ta, Th, U, Y, Z, and rare-earth elements (REE). The REE composition and chondrite-normalized patterns of LSS [low  $\sum$ REE (20–68 mg kg<sup>-1</sup>) and low La<sub>N</sub>/Yb<sub>N</sub> (1.9–7.4)]—are compatible with ultramafic-derived soils. The HSS samples display distinct REE composition with high  $\sum$ REE (102–336 mg kg<sup>-1</sup>) and La<sub>N</sub>/Yb<sub>N</sub> (13–51) which would be originated from granitoid, metamorphic, and sedimentary derived soils. The available percentage of heavy metals in the park soils is much higher than natural samples. The Pb characteristics of park soils are distinct from natural soils. These samples are less radiogenic than natural soils with lower <sup>206</sup>Pb/<sup>204</sup>Pb, <sup>207</sup>Pb/<sup>204</sup>Pb, <sup>208</sup>Pb/<sup>204</sup>Pb, <sup>206</sup>Pb/<sup>207</sup>Pb, and higher <sup>208</sup>Pb/<sup>206</sup>Pb ratios. The calculated contributions of possible sources in Mashhad park soils release 6.6 and 93.4% for natural and anthropogenic (industrial and leaded petrol) sources, respectively. The central parks exhibit the highest pollution of heavy metals in Mashhad indicating high traffic intensity in this area. The concentration of potentially toxic elements in the surface soils of Mashhad parks is lower than the national maximum permissible concentration, but many of them such as Cd, Cu, Mo, Pb, Sn, Se, and Zn are highly enriched relative to non-urban soils.

**Keywords** Geochemistry · Soil · Urban parks · Mashhad · Iran

## Introduction

Urban areas have wide anthropogenic impress on the environment. Urban soil acts as an important reservoir for accumulation of human-induced pollutants in the urban areas.

**Electronic supplementary material** The online version of this article (<https://doi.org/10.1007/s12665-018-7684-z>) contains supplementary material, which is available to authorized users.

✉ Seyed Ali Mazhari  
ali54894@yahoo.com; s\_mazhari@pnu.ac.ir

- <sup>1</sup> Department of Geology, Payame Noor University, Tehran 19395-4697, Iran
- <sup>2</sup> Faculty of Geography and Environmental Science, Hakim Sabzevari University, Sabzevar, Iran
- <sup>3</sup> Cellular and Molecular Research Center, Sabzevar University of Medical Sciences, Sabzevar, Iran

The chemical changes in urban soils are emanated by different factors such as industrial, traffic and domestic emissions, construction and atmospheric deposition. Therefore, urban soils differ greatly and demonstrate more variations than natural soils (Morel et al. 2015). The study of urban soils and their geochemical traits has grown in recent years, but many of these studies focused on the risk assessment of heavy metal concentrations (e.g., Andersson et al. 2010; Yang et al. 2011, 2014; Kelepertzis and Argyraki 2015; Horvath et al. 2016; Bourliva et al. 2017). Urban effects on the soil geochemistry are not limited to the heavy metals and other elements could be changed by urbanization, too. The abundance measurement of element contents and their chemical trends are used to obtain the properties, origin and geochemical evolution in the urban soil systems (Alekseenko and Alekseenko 2014).

Mashhad is the second super-city in Iran and has more than 3 million residents and over 20 million annual

pilgrimage tourists. This city is surrounded by numerous factories and the high growth of urbanization led to high air pollution, so that Mashhad had 92 day impure air with AQI (air quality index) > 200 in 2016 (EPMC 2017). Recent data on Mashhad plain (urban area includes a small part of this plain) indicate that the concentration of Zn, Ni, and Pb in the urban area is higher than background values (Karimi et al. 2017). The comprehensive geochemical characteristics of the soil samples in Mashhad parks will be defined in this study, which would be the first scientific work in this regard at Mashhad urban area. The similarities and differences between natural and park soils, anthropogenic, and lithogenic origin of elements and bioavailability and environmental assessment of Mashhad urban soils will be discussed in this article.

## Materials and methods

### Study area

Mashhad city is located at the NE of Iran ( $36^{\circ}14'–36^{\circ}22'N$  latitudes– $59^{\circ}29'–59^{\circ}41'E$  longitudes) and is the capital of the Khorasan Razavi province. This area falls in the northeastern slopes of Binaloud Mountains and is dominated by relatively flat topography with an altitude of 950–1150 m. This region is situated in Binaloud Zone (between Central Iran and Kopeh Dagh zones: Fig. 1a). The Binaloud Zone includes Paleo-Tethys remnants and is composed of structurally deformed ophiolitic rocks and low-to-medium-grade metamorphosed rocks. This zone was produced by obduction of the Paleo-Tethys oceanic crust over the Iranian microcontinental margin during terrane accretion (Alavi 1991). Metamorphic rocks (layered slate, phyllite, schist, marble, and carbonate meta-conglomerate of Permian age) encompass ophiolitic rocks. Alavi (1979, 1991) suggested a deep-water setting such as turbidite deposits for the original sedimentary environment of Binaloud Zone, which formed in a trench—forearc basin over a north-dipping subduction zone. In addition to these rock units, granitoid rocks are widespread in the Mashhad area. They outcrop as a large batholith to the south of Mashhad and a smaller isolated stock to the northwest of the city (Fig. 1b). These batholite and stocks consist of complex plutonic rocks which intruded during arc-related activity in late-Triassic (Mirnejad et al. 2013). Granitic, ultramafic, and meta-sedimentary rocks are the main lithological units which appear in the west–south of the city. The north and east sections of Mashhad city are covered by alluvium deposits (Fig. 1b).

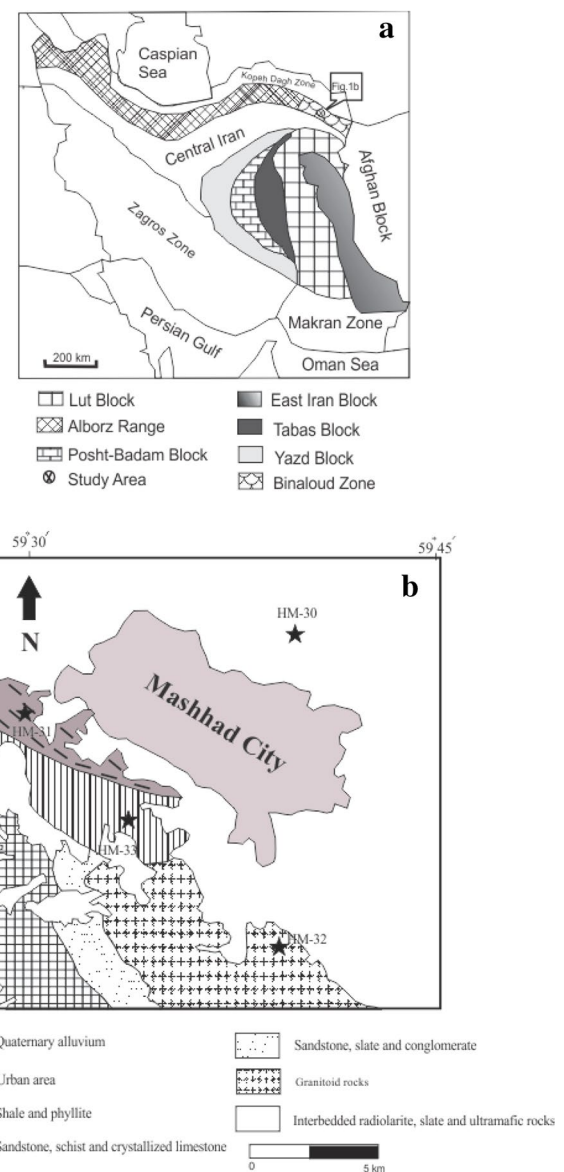


**Fig. 1** **a** Geological map showing tectonic units of Iran (modified after Nabavi 1976). **b** Simple map which illustrates lithological units of the study area. (modified from Taheri and Ghaemi 1994)

### Sampling and analysis

The main aim of this work focused on the urban areas of Mashhad to study park soil geochemistry. For this purpose, 23 parks were selected. At each selected park, top-soils (5–20 cm) were collected by a stainless-steel hand trowel. Each sample (average weight of 3 kg) was taken by mixing of five subsamples. For each park, 1 kg of soil was prepared from the mixed samples using a quartile method. In addition to park samples, four soil samples were collected from areas which were far from the urban

range and considered to be unpolluted (after this would be named as non-urban samples). The position of these samples is shown in Fig. 1b. The sample of HM-30 was taken from Sisabad village which considered as a pristine area for main soil supply in some parks of Mashhad. The samples of HM-31, HM-32, and HM-33 collected from in-situ soils derived from ultramafic, metamorphic, and granitoid rocks, respectively. These samples were used to compare urban and non-urban soils and define pollution and the original source of Mashhad park soils. Finally, 27 soil samples were stored in polyethylene bags for transport and storage. Each sample was air-dried and sieved to separate the < 2-mm fraction for geochemical analyses. To get a better understanding of soil chemistry, parameters of pH and total organic carbon (TOC) were determined.

To measure soil pH, a solution of water and 1 M KCl with 1:2.5 ratio of soil/solution was used. The TOC was measured by the Modified wet oxidation method (Walkley–Black). Soil samples, after being sieved to < 2 mm, were ground to fine powder (< 180 nm). All samples were analyzed for major and 48 trace elements, including 14 rare-earth elements (REE). Total major oxides and trace elements of the soil samples were determined by X-ray fluorescence (XRF) and inductively coupled plasma mass spectrometry (ICP-MS), respectively. These analyses were done at the accredited Activation Laboratories (ActLabs.), Canada. The XRF performed after fusion with lithium tetraborate. Precision was calculated on in-house replicates and 20 blind duplicates. Typical precision was better than  $\pm 1.5\%$  for an analyte concentration of 10 wt%. For ICP-MS analysis, a multi-acid digestion procedure was used. In this method, 0.25 g of the soil sample was heated in a mix of HF–HNO<sub>3</sub>–HClO<sub>4</sub> to fume and made it dry. Then, the residue was dissolved in HCl. The accuracy of analyses was evaluated by quality assurance and quality control (QA/QC) included reagent blanks, analytical duplicates, and analyses of in-house reference materials (multi-element soil standards GXR-1, GXR-4, GXR-6, SDC-1, OREAS 45d, and SdAR-M2). The blanks method results were totally below the detection limits. The recovery rates were estimated within  $\pm 10\%$  of the certified value, and analytical precision was better than  $\pm 5\%$ .

To determine labile and bioavailable fraction of heavy metals (Cd, Co, Cr, Cu, Ni, and Pb), the modified BCR sequential extraction (European Community Bureau of Reference) was applied to determine four fraction concentrations in the soil samples: weak-acid soluble ( $F_1$ ), reducible ( $F_2$ ), oxidizable ( $F_3$ ), and residual ( $F_4$ ) fractions (Rauret et al. 2000; Ferri et al. 2012). In the first step, a 40 mL of 0.11 M acetic acid was used to extract weak-acid-soluble (the exchangeable and carbonates fraction) metals. Then, 40 mL of 0.5 M hydroxylammonium chloride was added to soil residue from the previous step at pH 1.5 to extract fraction 2. Next, the solution of 20 mL of 8.8 M hydrogen peroxide and

50 mL of 1.0 M ammonium acetate was added to soil residue to extract fraction 3. In the last step, the residual soils were digested in 5 mL of 7.5 N HNO<sub>3</sub> at 80 °C and fraction 4 was extracted. In each step, the filtrate was analyzed for heavy metals by flame atomic absorption spectrometer (FAAS). BCR-100 standard was used to determine the precision and accuracy of element concentration analysis. The precision which determined after three repeated measurements was  $\pm 5\%$ . The detection limits of heavy metals defined by ICP-MS were not profit (Table 1, Supplementary). Therefore, the total concentration of Cd, Cr, Co, Cu, Ni, and Pb was analyzed by FAAS.

The Pb isotopes were measured in all samples by a Thermo-Finnigan Neptune high-resolution multi-collector inductively coupled-plasma mass spectrometry (MC-ICP-MS). A mixed acid solution of HF + HClO<sub>4</sub> + HNO<sub>3</sub> was used to digest powdered samples. Afterward, the solution was heated in 45 ml ultra-clean PFA digestion vessels to remove silicate fraction and then dissolved it with HCl and HBr, and the digestion solution was diluted to a final Pb concentration of ca. 2 ng/ml with 2% high-purity HNO<sub>3</sub>. The extracted Pb was re-purified in an AG1 × 8 anion-exchange column. To correct mass bias, Tl spike to each sample was added using the <sup>205</sup>Tl/<sup>203</sup>Tl value of 2.3875. Mass fractionation was closely checked by continuous analysis of the NIST standards under identical running conditions as samples. The values measured for the NIST 981 standard were  $16.9411 \pm 0.001$ ,  $15.4958 \pm 0.0008$ ,  $36.7216 \pm 0.003$  and  $2.1677 \pm 0.00008$  ( $1\sigma$ ) for <sup>206</sup>Pb/<sup>204</sup>Pb, <sup>207</sup>Pb/<sup>204</sup>Pb, <sup>208</sup>Pb/<sup>204</sup>Pb, and <sup>208</sup>Pb/<sup>206</sup>Pb, respectively. Analytical uncertainties for Pb were calculated as the relative standard deviation of 20 replicate samples. The precision ( $1\sigma$ ) was 0.06% for <sup>206</sup>Pb/<sup>204</sup>Pb, 0.05% for <sup>207</sup>Pb/<sup>204</sup>Pb, 0.08% for <sup>208</sup>Pb/<sup>204</sup>Pb, and 0.02% for <sup>208</sup>Pb/<sup>206</sup>Pb.

To perform chemical analyses, deionized water (with 16–17 MΩ cm<sup>-1</sup> resistivity) and Sigma-Aldrich ACS grade products were used. The purity of these reagents was as follows: HNO<sub>3</sub> ( $\geq 90\%$ ), HF ( $\geq 48\%$ ), HCl (37%), HBr (48%), acetic acid ( $\geq 99.8\%$ ), HClO<sub>4</sub> (70%), KCl ( $> 99\%$ ), hydroxylammonium chloride (99%), hydrogen peroxide ( $> 30$ ), and ammonium acetate (99.9%).

Pearson correlation coefficients and principal component analysis (PCA) are used to investigating elemental associations and extract latent factors for analyzing relationships among the observed variables (Yang et al. 2011; Argyraki and Kelepertzis 2014). In this regard, the statistical analyses of park soils data were done with SPSS 16.0 for Windows software. PCA was performed via Varimax with the Kaiser normalization rotation method. This method considers only factors with eigenvalues  $> 1$  and minimizes the number of variables, so that the interpretation of output results would be facilitated (Bourliva et al. 2017). The geochemical maps were plotted by a geographical information system (GIS)

**Table 1** Principle component analysis (PCA) of geochemical variables for park soils of Mashhad city

	Rotated component matrix <sup>a</sup>				
	PC1	PC2	PC3	PC4	PC5
SiO <sub>2</sub>	-0.898	-0.168	-0.268	-0.216	-0.084
Al <sub>2</sub> O <sub>3</sub>	-0.927	0.230	-0.054	-0.088	-0.225
FeO <sub>t</sub>	0.944	-0.041	-0.095	-0.044	0.109
MgO	0.945	0.172	0.198	0.960	0.062
CaO	0.311	0.280	0.894	0.056	0.070
Na <sub>2</sub> O	-0.355	-0.128	-0.117	-0.465	0.236
K <sub>2</sub> O	-0.033	0.159	0.094	0.945	0.057
Ag	0.890	0.171	0.322	-0.012	0.066
As	0.907	0.213	0.262	0.086	0.077
Ba	0.380	0.217	0.861	0.112	0.123
Cd	0.116	0.958	0.178	-0.007	0.071
Co	0.825	0.447	0.264	0.127	0.034
Cr	0.928	0.317	0.100	0.097	0.066
Cu	0.550	0.791	0.048	0.073	-0.017
Ga	-0.947	-0.160	-0.182	-0.033	-0.116
Hf	-0.920	-0.171	-0.130	0.059	0.181
Li	-0.845	-0.347	-0.213	-0.056	-0.106
Mn	0.886	0.137	0.218	-0.280	-0.020
Mo	0.050	0.976	0.117	0.074	-0.025
Nb	-0.804	-0.333	-0.328	0.054	-0.028
Ni	0.863	0.412	0.134	0.058	0.090
P	-0.195	-0.134	-0.079	-0.090	-0.914
Pb	0.166	0.952	0.111	0.119	0.041
Rb	-0.113	0.127	-0.007	0.922	0.136
S	0.937	0.184	0.223	0.028	0.024
Sb	0.942	0.197	0.193	0.048	0.013
Sc	0.955	-0.002	0.112	-0.008	0.029
Se	0.185	0.950	0.021	0.145	0.004
Sn	0.107	0.974	0.144	0.102	0.009
Sr	0.301	0.257	0.892	0.009	-0.075
Ta	-0.957	-0.047	-0.181	-0.086	-0.036
Th	-0.915	-0.155	-0.307	-0.092	0.077
Ti	0.892	0.122	0.312	-0.214	0.083
U	-0.830	-0.119	-0.392	-0.226	0.061
V	0.943	0.068	-0.003	-0.123	0.078
Y	-0.925	-0.188	-0.222	0.068	0.069
Zn	0.177	0.945	0.186	0.019	0.090
Zr	-0.939	-0.132	-0.031	-0.018	0.176
∑REE	-0.642	0.038	-0.550	-0.085	-0.012
% Variance explained	54.174	19.260	10.143	6.090	3.004
Cumulative % variance	54.174	73.434	83.576	89.666	92.670

<sup>a</sup>Rotation method: Varimax with Kaiser normalization

using ArcMap v.10.0 (ArcGIS) to show the overall spatial distribution patterns of total and available heavy metal concentrations. For the drawing of maps, the inverse distance weighted (IDW) interpolation method with a power of 2 was used.

## Results and discussion

### Major and trace-element composition of soils

The major oxides and trace-element concentration of the studied soils along with their pH and TOC values are listed in Supplementary Table 1. All soils have weakly alkaline pH values (7.72–9.11) and low TOC range (<2.2% in non-urban soils and 2–5.5% in park soils). The pH and TOC variability in soil samples are limited and there is not any meaningful relation between pH–TOC and element concentrations. Therefore, these parameters did not have a major role in the geochemical evolutions of Mashhad soils.

In non-urban samples, the element concentrations in Sisabad soil (HM-30), granitoid-derived soil (HM-32), and metamorphic rock-derived soil (HM-33) are similar, while ultramafic-derived soil (HM-31) shows distinctive composition. The first three samples have a higher concentration of SiO<sub>2</sub>, Al<sub>2</sub>O<sub>3</sub>, Na<sub>2</sub>O, K<sub>2</sub>O, Ba, Ga, Hf, Li, Nb, P, Sn, Ta, Th, U, Y, and REE than the HM-31. On the other side, ultramafic soil shows the higher content of FeO<sub>t</sub>, MgO, Ag, Co, Cr, Cu, Mn, Ni, S, Sb, Ti, and V relative to other non-urban samples (Supplementary Table 1).

The chemical composition of Mashhad parks soils shows striking changes between different samples. By detail consideration of analytical data, the soils of Mashhad parks could be divided into two groups: high silica soils (HSS) and low silica soils (LSS). These two groups have mean SiO<sub>2</sub> values of 53.93 and 47.57 wt%, respectively. The mean concentration of MgO (7.07 wt%), FeO<sub>t</sub> (6.25 wt%), As (4.66 mg kg<sup>-1</sup>), Co (31.28 mg kg<sup>-1</sup>), Cr (206.26 mg kg<sup>-1</sup>), Cu (83.08 mg kg<sup>-1</sup>), Mn (937 mg kg<sup>-1</sup>), Ni (167.76 mg kg<sup>-1</sup>), Pb (112.13 mg kg<sup>-1</sup>), S (1612 mg kg<sup>-1</sup>), Sc (16.35 mg kg<sup>-1</sup>), Sn (22.26 mg kg<sup>-1</sup>), Ti (8158 mg kg<sup>-1</sup>), V (75.41 mg kg<sup>-1</sup>), and Zn (166.5 mg kg<sup>-1</sup>) in LSS are significantly higher than HSS with mean values of MgO (4.08 wt%), FeO<sub>t</sub> (4.07 wt%), As (3.87 mg kg<sup>-1</sup>), Co (18.61 mg kg<sup>-1</sup>), Cr (119.12 mg kg<sup>-1</sup>), Cu (57.23 mg kg<sup>-1</sup>), Mn (366 mg kg<sup>-1</sup>), Ni (110.2 mg kg<sup>-1</sup>), Pb (87.6 mg kg<sup>-1</sup>), S (1180 mg kg<sup>-1</sup>), Sc (9.71 mg kg<sup>-1</sup>), Sn (15.49 mg kg<sup>-1</sup>), Ti (3595 mg kg<sup>-1</sup>), V (23.45 mg kg<sup>-1</sup>), and Zn (125.4 mg kg<sup>-1</sup>). On the other hand, The HSS samples have a higher content of SiO<sub>2</sub>, Ga, Li, Nb, Ta, Th, U, Y, Zr, and REE than LSS samples. These differences could be elegantly demonstrated in binary diagrams (Fig. 2).

The spatial variation of some heavy metals concentrations in park soils is shown in Fig. 3. There is a clear correlation between metal distributions, so that central parks generally have higher content in all heavy metals that could be related to high traffic and air pollution in these areas.

### The comparison of park soils and non-urban soils

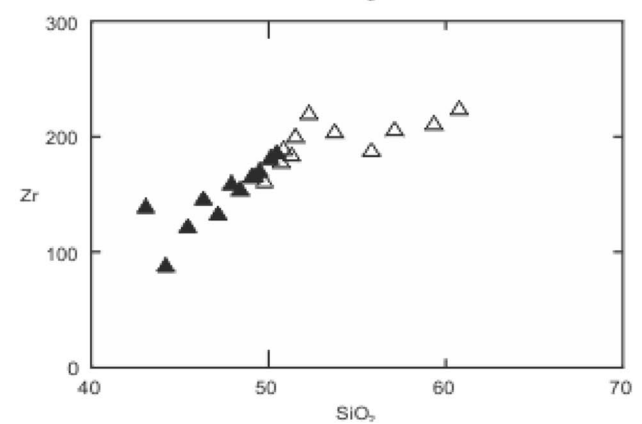
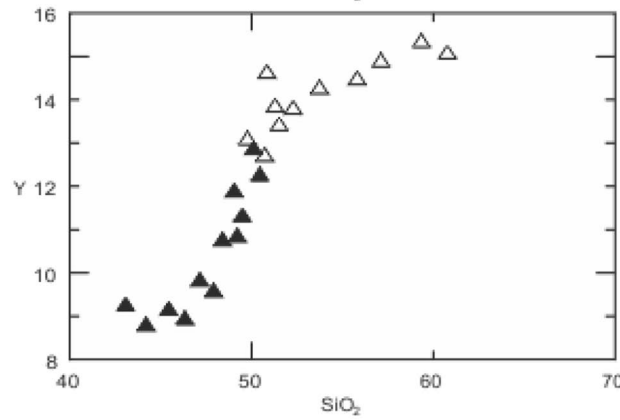
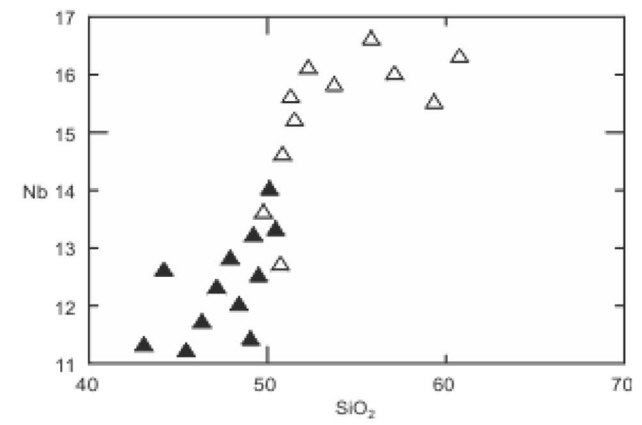
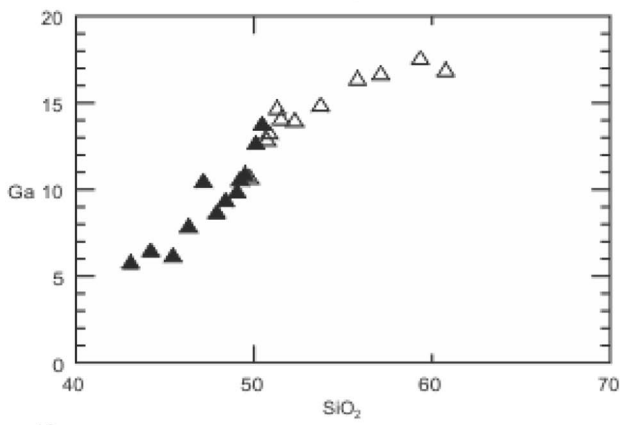
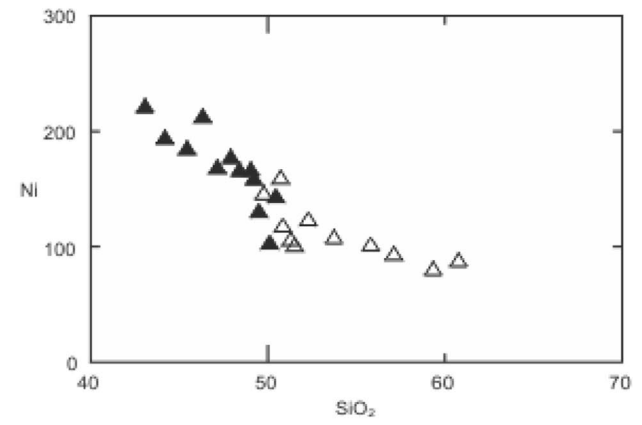
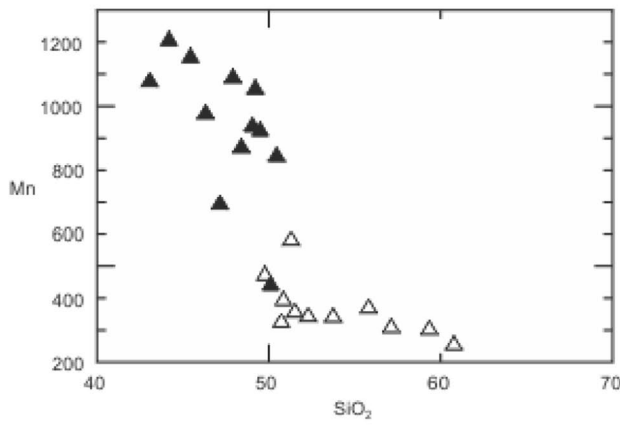
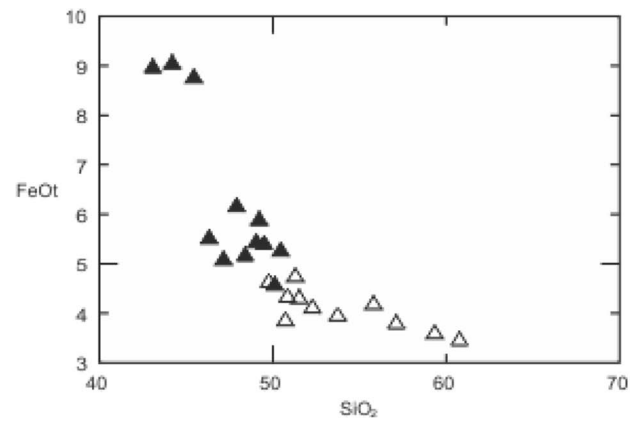
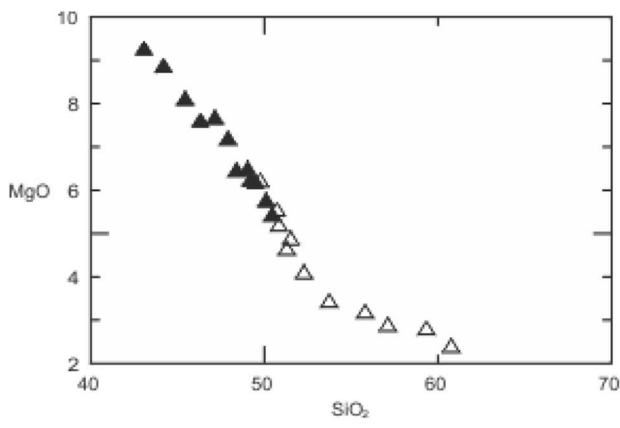
The soil samples collected from Mashhad parks are remarkably enriched in some elements, especially heavy metals. These soils contain higher concentrations of As, Cd, Cu, Mo, P, Pb, S, Sb, Se, Sn, and Zn than non-urban soils (Fig. 4). In several park samples, the enrichment of some elements such as Pb and Cd is more than ten times of non-urban soils (Fig. 4). These data indicate that urbanization growth of Mashhad city is the most important factor in the accumulation of these elements. The concentration of Co, Cr, and Ni in Mashhad parks is notably higher than three samples of non-urban soils (HM-30, HM-32, and HM-33). The only exception is the ultramafic-derived soil (HM-31) which is highly concentrated in Co, Cr, and Ni (Supplementary Table 1). The soils derived from ultramafics (peridotite or serpentinite rocks) normally have high concentrations of these three elements (Alexander 2004). This issue is also obvious in other ultramafic derived soils of Khorasan province (Mazhari et al. 2013, 2017). Therefore, the origin of Cr, Co, and Ni in the soils of Mashhad parks could be both of anthropogenic or lithogenic sources. This subject will be discussed in the next sections.

The rare-earth elements (REE) are used to interpret geochemical phenomena such as earth's crust evolutions, the genesis of rocks and minerals and sediment origin (e.g., Rollinson 1993). The use of REE in the studying of soil weathering and pedogenetic processes has been increased in recent years (e.g., Schilling et al. 2014; Mazhari and Sharifiyan Attar 2015; Jin et al. 2017). Although REE are used in some materials (batteries, computer monitors, catalysts, fiber-optic telecommunication cables, etc), they are considered to have a natural origin and derived mostly from the soil parent material. However, other sources (such as fertilizers and atmospheric emissions) may impress on the REE composition (Giusti 2013). The REE composition of Mashhad soils displays interesting differences between various samples. In non-urban soils, ultramafic-derived soil has lower REE abundance ( $\sum \text{REE} = 11.50 \text{ mg kg}^{-1}$ ) relative to other samples ( $\sum \text{REE} = 191.45\text{--}391.23 \text{ mg kg}^{-1}$ ). Furthermore, chondrite-normalized REE diagram trends are different between ultramafic and other non-urban soils (Fig. 5a). The ultramafic soil (HM-31) shows W-like pattern with depleted LREE ( $\text{La}_N/\text{Yb}_N = 0.73$ ) and positive Eu anomaly ( $\text{Eu}/\text{Eu}^* = 1.22$ ), while the other samples exhibit more evolved REE patterns with enriched LREE ( $\text{La}_N/\text{Yb}_N = 13\text{--}49$ ) and slight negative Eu anomaly ( $\text{Eu}/\text{Eu}^* = 0.8\text{--}0.9$ ) (Fig. 5a). The variation of REE

content in Mashhad parks soils is more extensive and HSS and LSS groups show different trends. The HSS group has a higher REE abundance ( $\sum \text{REE} = 102\text{--}336 \text{ mg kg}^{-1}$ ) than LSS ( $\sum \text{REE} = 20\text{--}68 \text{ mg kg}^{-1}$ ). These two groups depict distinct patterns in the chondrite-normalized REE diagrams, too (Fig. 5b, c). In a general respect, the REE patterns of LSS are more similar to the HM-31 sample, while HSS samples have REE patterns near to the other non-urban soils. However, the REE patterns of park soils are not so regular and show wide variation, especially in LSS group (Fig. 5c). The addition of fertilizers and high content of clay minerals would lead to change REE concentration of serpentine and ultramafic-derived rocks (Mazhari and Sharifiyan Attar 2015). This issue is true about LSS samples. Furthermore, the geochemical compositions of LSS samples and HM-31 are not completely the same (Supplementary Table 1), but it should be said that ultramafic rocks had more influence in the REE content of LSS group. Urbanization and mixing with other soils are the most important factors which make the difference between LSS and HM-31 samples.

### Statistic assessment of geochemical data in the park soils

Principle component analysis (PCA), as the most applicable multivariate statistical method in the environmental studies, is an effective technique to identify the source of trace elements in soils (Loska and Wiechuya 2003; Reid and Spencer 2009; Gu et al. 2016). In this study, PCA was performed on 23 samples of Mashhad soil parks and the results, including factor loadings, are presented in Table 1. Five principal components (PC) with eigenvalues  $> 1$  were determined which explain 92.67% of total variance. The first component (PC1) is the main component which accounted for 54.17% of total variance. This component shows two different associations (Table 1): (1) elements with strong positive factor loadings ( $\text{FeO}_r$ , MgO, Ag, As, Co, Cr, Mn, Ni, S, Sb, Sc, Ti, and V) and (2) elements with strong negative factor loadings ( $\text{SiO}_2$ ,  $\text{Al}_2\text{O}_3$ , Ga, Hf, Li, Nb, Ta, Th, U, Y, Zr, and REE). The results of Pearson correlation coefficients and binary diagrams affirm the same adverse relations between these two groups (Table 2; Fig. 2). These associations are in accordance with natural geochemical trends, so PC1 could be considered as the natural source component which is originated from parental materials. The elements of Cd, Cu, Mo, Pb, Se, Sn, and Zn have strong positive loads in PC2, which accounted for 19.26% of the total variance (Table 1). They also show strong correlation coefficients (Table 2). This component includes typical urban contamination indicators (i.e., Cd, Cu, Pb, and Zn) and may reflect anthropogenic pollution of park soils. The positive factor loadings of CaO, Ba, and Sr in PC3 could be interpreted as the influence of calcareous content in soil samples. PC3



◀**Fig. 2** Binary diagrams show the relation of  $\text{SiO}_2$  (in wt%) v. other elements (in  $\text{mg kg}^{-1}$ ) in the soil samples of Mashhad parks. Note the different trends of metals (positive correlations) and HFSE (high field strength elements; negative correlations). Filled triangle: LSS, open triangle: HSS

accounted for 10.14% of the total variance (Table 1). In the last two components, positive factor loadings of  $\text{K}_2\text{O}$  and Rb (in PC4) and negative loading of P (in PC5) were extracted (Table 1). These components accounted for < 10% of the total variance and may be resulted by complex natural and anthropogenic sources.

### The BCR sequential extraction

Although the total concentration of trace elements has been used in many studies to define environmental risk assessments in the soils, it is recognized that the toxicity and environmental effects are essentially related to the mobility and availability of these elements (Liu et al. 2015). The total concentration of elements is not a suitable indicator of bioavailability, mobility, or toxicity, because these characteristics are mainly depending on the different chemical forms of binding between trace elements and solid phases of the samples (Ferri et al. 2012). To investigate the trace element (especially heavy metals) availability and mobility in soils, a number of extraction methods have been extensively used (Liu et al. 2015). Different studies suggest that the sequential extraction method could be an important and useful approach (Ure and Davidson 1995). In this study, the BCR sequential extraction was applied to define toxicity and bioavailability of six soil heavy metals (Cd, Co, Cr, Cu, Ni, and Pb) in Mashhad urban and non-urban soils. These heavy metals were selected, because they display two different groups in the PCA diagram (Fig. 6). Four fractions that extracted in this method have different availability: the exchangeable and carbonates forms ( $F_1$ ) are considered as the most labile fraction. Reducible bounded to Fe/Mn oxides ( $F_2$ ) and oxidizable bounded to organic matters ( $F_3$ ) are less mobile, but may be potentially available, while the residue bounded to the soil matrix ( $F_4$ ) is not labile and is known as an unavailable fraction (Rodríguez et al. 2009). Therefore, the  $F_1$  content (the most labile fraction) and the sum of  $F_1$ ,  $F_2$  and  $F_3$  fractions (non-residual or potentially available fraction) are considered as effective parameters in the environmental availability of Mashhad soils. The results of BCR sequential extraction are presented in Supplementary Table 2.

### Cadmium

The concentration of the most labile fraction ( $F_1$ ) of Cd in non-urban soils is lower than detection limit and the average

potentially available of these soils is 26% of total Cd content. In contrast, Mashhad park soils show various  $F_1$  content which differs from less than 12% to more than 42% of total Cd concentration. The average Cd in  $F_1$  and ( $F_1 + F_2 + F_3$ ) fractions of park soils are 26 and 72% of the total Cd, respectively. There is a positive correlation between the total and available fraction of Cd concentration (Fig. 7a). As it is clear, the park soils reveal very high availability that would be resulted by anthropogenic pollution. The most concentration of available Cd occurred in the soil samples of central parks (Fig. 8a) which have > 90% of available Cd (Supplementary Table 2).

### Cobalt

In the non-urban soil samples, Co is mainly associated with residual ( $F_4$ ) fraction (average 78% of total Co). The Co availability is similar in all non-urban soils, so that  $F_1$  fraction is composed of < 6% of total Co and available concentration of cobalt is low. The highest measured non-residual Co is 18.25 ppm in the serpentine derived sample (Supplementary Table 2).

The variance of the exchangeable fraction in urban samples is obvious (6.4–24% of total Co) and the non-residual fractions constitute 32–60% of total Co. The positive correlation of total and available fraction of cobalt in Mashhad park soils are more irregular (Fig. 7b). The distribution of non-residual Co in park samples (Fig. 8b) exhibits somewhat different pattern relative to total Co (compare Fig. 3).

### Chromium

The non-residual fractions of Cr in non-urban soil samples form less than 1% of total Cr. Therefore, Cr could be considered as a non-available element in these soils. The highest Cr chemical partitioning percentages of park soils occurred in residual fraction, too (average 74% of total Cr). However, the soils exhibit palpable differences in the distribution of non-residual Cr (17–49% of total Cr). The total and non-residual association is negative for Cr concentration of park soils (Fig. 7c). The soil samples with higher non-residual Cr appeared in the southern parks of Mashhad (Fig. 8c).

### Copper

The non-urban soil samples release 7–8 and 23–24% of total Cu in the  $F_1$  and non-residual fractions, respectively (Supplementary Table 2). The exchangeable fraction of park soils is more than three times of non-urban samples (15–26%) and non-residual fractions include 48–90% of total Cr in these soils (Fig. 7d). The highest values of potentially available Cu are visible in the central park soils of Mashhad (Fig. 8d), which has good relevance to total Cu distribution (Fig. 3).

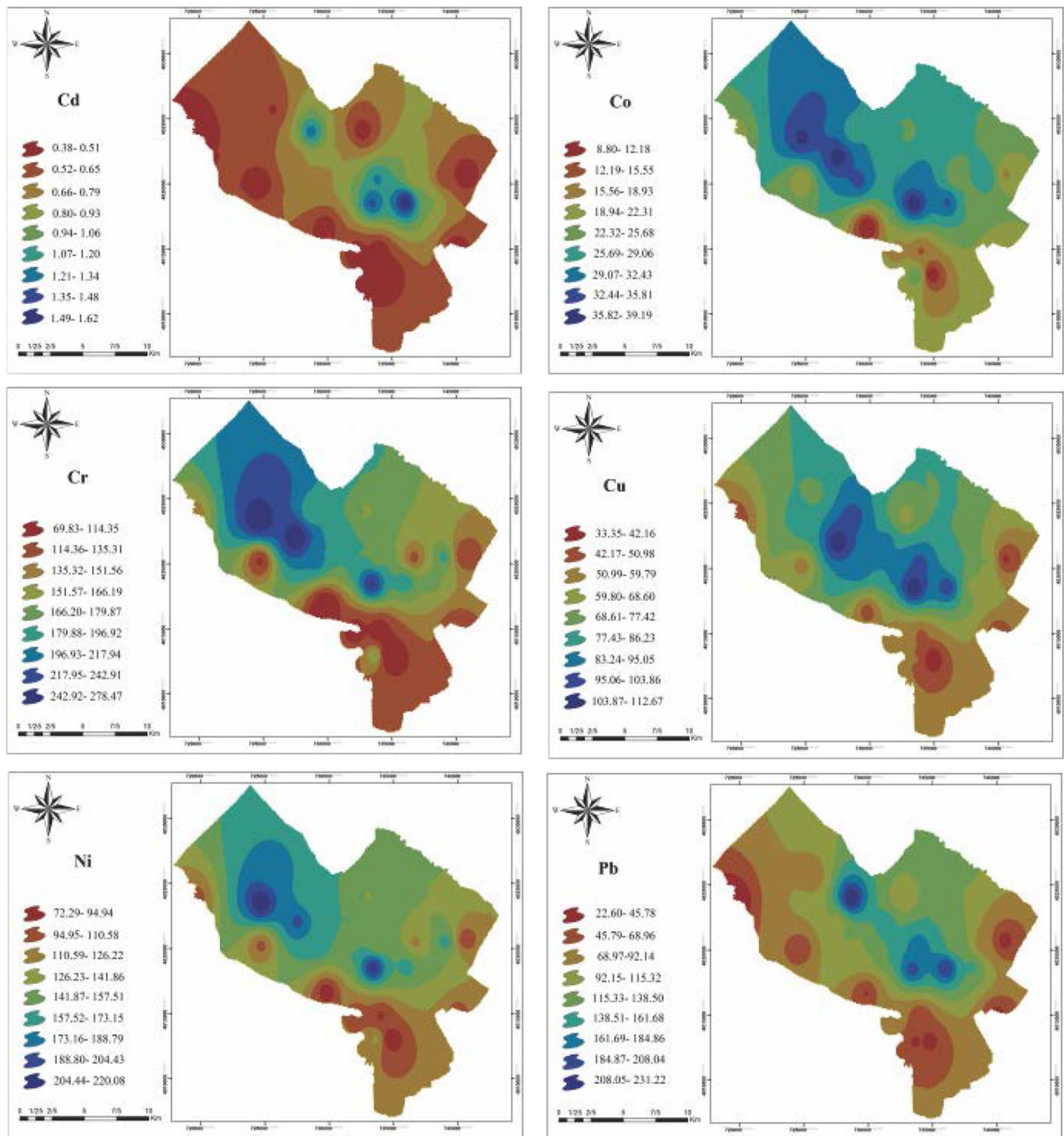


**Fig. 3** Spatial distribution of heavy metal concentrations in the soil samples of Mashhad parks

### Nickel

The labile percentage of Ni in the non-urban soils is as low as 5–6% of total Ni (Table 4). These samples have 7–216 mg kg<sup>-1</sup> concentrations in the non-residual fractions (20–22% of total Ni). The labile and potentially

available fractions in park soils increase to 9–20 (average 13%) and 33–61% (average 43%) of total Ni, respectively. The correlation between non-residual fractions and total Ni is negative similar to Cr (Fig. 7e). The distribution pattern of non-residual fractions of Mashhad soil parks (Fig. 8e) is different from total Ni (Fig. 3).



## Lead

Similar to other heavy metals, Pb in the exchangeable fraction of non-urban soils is fairly small (5–7% of total Pb). The potentially available fractions vary between 22 and 32% of total Pb in these soils. The labile fraction of Pb in urban soils includes 15–34% (average 30% of total Pb). The soil samples of Mashhad parks show high available Pb (67–93%, average 87% of total Pb), which positively related to the total Pb (Fig. 7f). Pb has the highest non-residual fractions relative to other heavy metals that is manifested in the distribution map (Fig. 8f).

As discussed above, park soil samples have higher available heavy metal contents than non-urban soils. The potentially available fractions of non-urban samples are more or less similar for all heavy metals (20–25% total concentration), with exception of Cr that is unavailable in these soils. On the other hand, the non-residual/total ratio is not the same for all extracted heavy metals in the park soils. The heavy metals of Pb, Cu, and Cd have high non-residual fractions, while Cr, Ni, and Co exhibit lower availability. High total concentration, strong association, and positive correlation between total and non-residual fractions testify to the anthropogenic origin of Pb, Cu, and Cd. As mentioned before, serpentinite derived soils (HM-31 sample) has high concentrations of Cr, Ni, and Co. Furthermore, PCA results show that these elements were included in PC1 which is thought to be derived from natural sources (“[Statistical assessment of geochemical data in the park soils](#)”). However, detailed consideration of PCA analysis indicates that although Co, Cr, and Ni have strong factor loadings in PC1, they also display moderate loadings (Co = 0.45; Cr = 0.32; Ni = 0.42) in PC2 (with anthropogenic source). Therefore, both anthropogenic and natural sources were involved in the Co, Cr, and Ni concentrations of Mashhad park soils.

## Lead isotope composition of soil samples

There are significant Pb isotopic differences between geogenic materials and pollutants comprising Pb of industrial origin (Pb ore). Pb ores have very high Pb/U and Pb/Th relative to ordinary rocks and consequently, their Pb isotopic content remained constant since their formation. Therefore, Pb ores are specified by distinguished, age dependent isotopic compositions with relatively unradiogenic signatures ( $^{206}\text{Pb}/^{204}\text{Pb}$  from 16 to 18.5, Hansmann and Köppel 2000). In contrast, Pb composition of unpolluted soils is originated from weathered bedrocks in which the Pb isotopic composition changed with time reflecting the U/Pb and Th/Pb of the parent rocks. Therefore, the Pb isotopic characteristics of unpolluted soils are generally more radiogenic ( $^{206}\text{Pb}/^{204}\text{Pb}$ : 18.5–19.5) than those of industrial Pb (Hansmann and Köppel 2000).

The Pb isotope ratios (Supplementary Table 3) vary in ranges between 1.206 and 1.237 ( $^{206}\text{Pb}/^{207}\text{Pb}$ ), 2 and 2.064 ( $^{208}\text{Pb}/^{206}\text{Pb}$ ), 38.681 and 38.839 ( $^{208}\text{Pb}/^{204}\text{Pb}$ ), 15.541 and 15.562 ( $^{207}\text{Pb}/^{204}\text{Pb}$ ), and 18.737 and 19.420 ( $^{206}\text{Pb}/^{204}\text{Pb}$ ) for the non-urban soils. These ratios vary between 1.1163 and 1.161 ( $^{206}\text{Pb}/^{207}\text{Pb}$ ), 2.1066 and 2.162 ( $^{208}\text{Pb}/^{206}\text{Pb}$ ), 37.405 and 37.964 ( $^{208}\text{Pb}/^{204}\text{Pb}$ ), 15.4823 and 15.5248 ( $^{207}\text{Pb}/^{204}\text{Pb}$ ), and 17.284 and 18.024 ( $^{206}\text{Pb}/^{204}\text{Pb}$ ) for the park soil of Mashhad. As it is clear from isotopic signatures, park soils show distinct composition from non-urban soils. These samples are less radiogenic than non-urban soils with lower  $^{206}\text{Pb}/^{204}\text{Pb}$ ,  $^{207}\text{Pb}/^{204}\text{Pb}$ ,  $^{208}\text{Pb}/^{204}\text{Pb}$ ,  $^{206}\text{Pb}/^{207}\text{Pb}$ , and higher  $^{208}\text{Pb}/^{206}\text{Pb}$  ratios. The wide range of isotope ratios in park soils indicates that the Pb content in the soils is produced by the combination of different sources including natural or anthropogenic origins and that it has also been accumulating over time because of the enormous use of Pb in fuel, industrial activities, etc. (Galušková et al. 2014). The low  $^{206}\text{Pb}/^{204}\text{Pb}$  values in park soils restate a possible anthropogenic origin from the use of fossil fuels (Komárek et al. 2008).

## Lead source identification

Different equations have been established for determining the contribution of possible Pb sources (natural or anthropogenic) by their contents and isotopic ratios (Li et al. 2011). The most prominent approach is the simple binary model which calculate the contribution of two end-members (i.e., natural or geogenic Pb vs. leaded petrol Pb) (Monna et al. 1999). Another approach is the three-end-member model which presents the information needed to identify possible sources of natural ( $F_1$ ), industrial emissions ( $F_2$ ), and leaded petrol ( $F_3$ ) emissions in soil samples by means of Pb content and isotopic ratios (Li et al. 2011). The contribution percentage of each source could be calculated according to the following three equations (Rodríguez-Seijo et al. 2015):

$$F_1 + F_2 + F_3 = 1$$

$$(F_1 \times R_1) + (F_2 \times R_2) + (F_3 \times R_3) = R_{\text{soil}}$$

$$(F_1/C_1) + (F_2/C_2) + (F_3/C_3) = 1/C_{\text{soil}}$$

In these equations,  $F_1$ ,  $F_2$ , and  $F_3$  are the contributions of natural, industrial and leaded petrol sources in the soils, respectively.  $R_1$  is the  $^{206}\text{Pb}/^{207}\text{Pb}$  ratios of natural (1.2252) source and  $R_2$ ,  $R_3$ , and  $R_{\text{soil}}$  are the  $^{206}\text{Pb}/^{207}\text{Pb}$  values of industrial (1.1427–1.1576), leaded petrol (1.097), and soil samples (Rodríguez-Seijo et al. 2015).

The Pb isotope ratios of non-urban soils are very radiogenic and have similar values to average content of the earth's continental crust ( $^{206}\text{Pb}/^{207}\text{Pb} = 1.20$ , Frostick et al. 2008). Therefore, these samples could be considered as

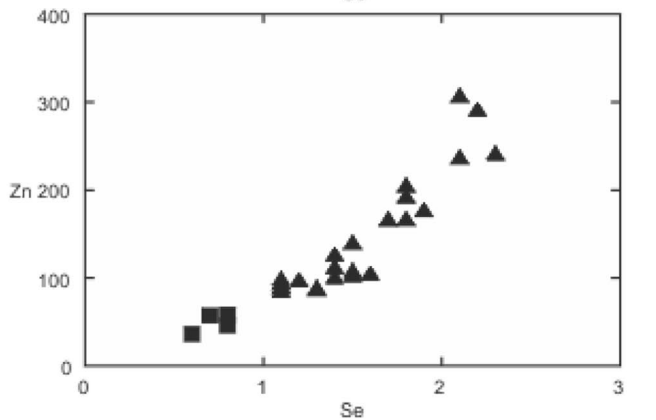
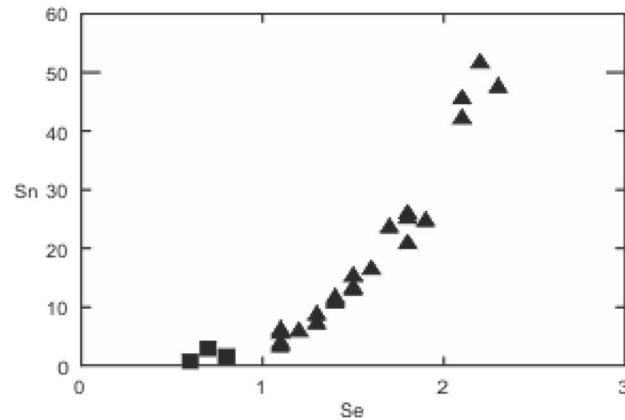
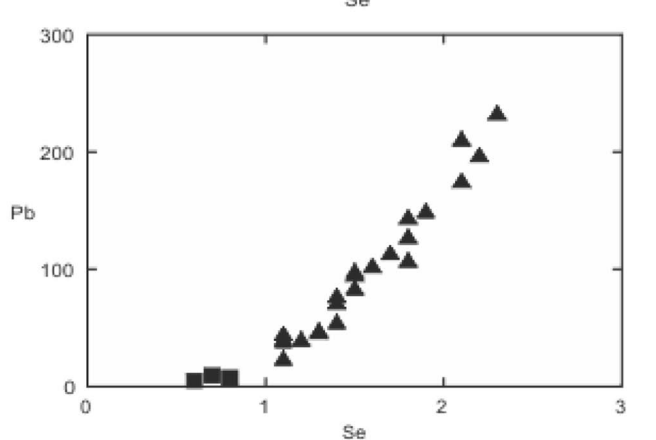
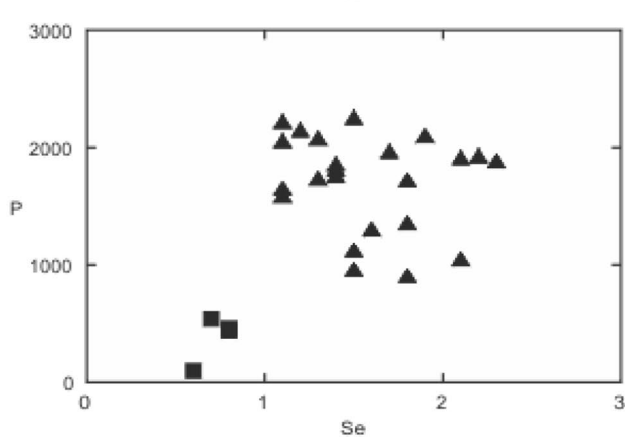
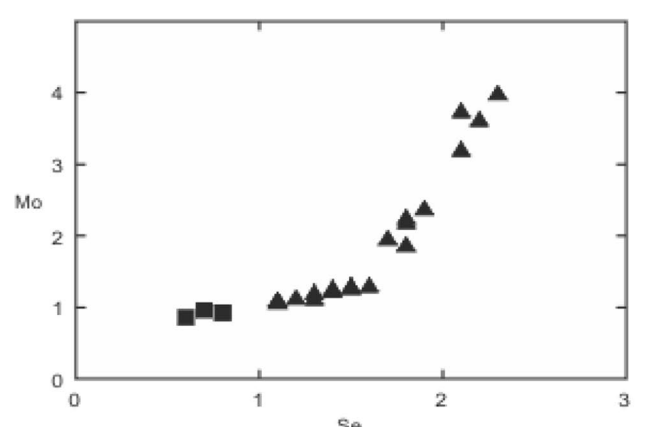
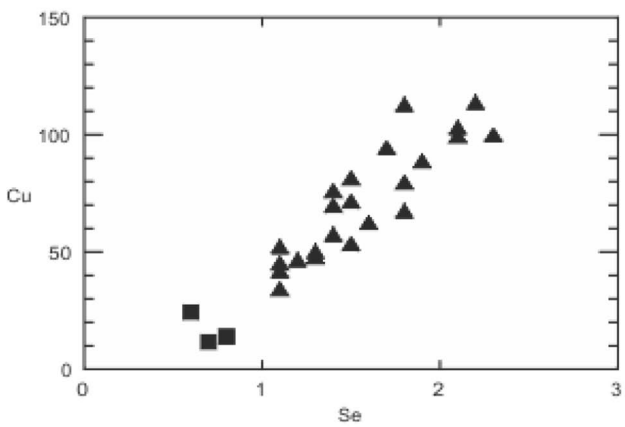
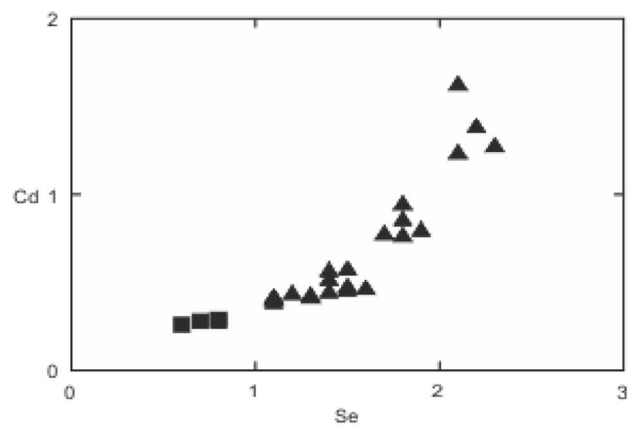
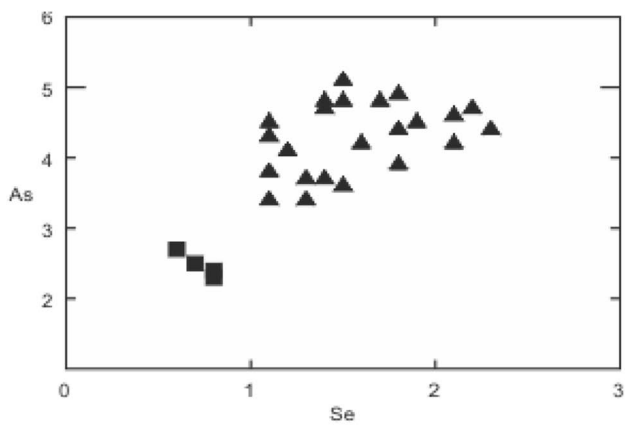


**Fig. 4** Binary diagrams of Se and other elements (in mg kg<sup>-1</sup>) illustrate composition differences between non-urban soils (filled square) and park soils (filled triangle) in Mashhad area

non-contaminated soils with natural or geogenic origin. The three-end-member model was used to determine possible Pb sources in the park soils of Mashhad. The calculated

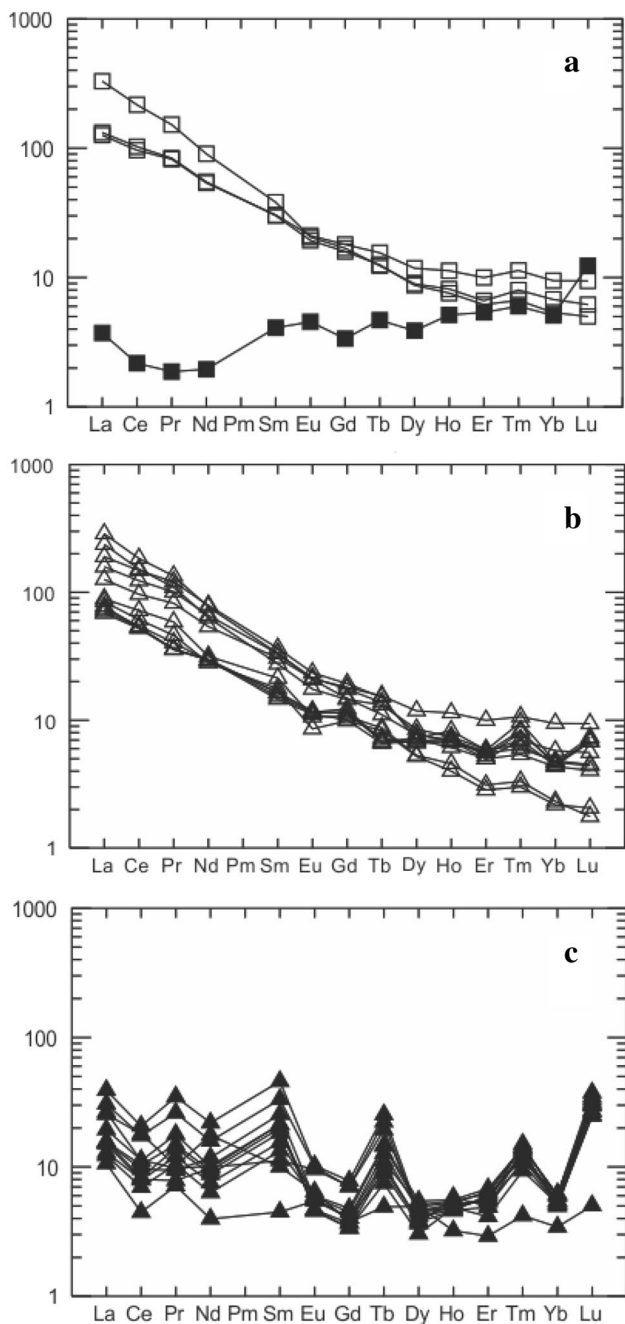


**Fig. 5** Chondrite-normalized REE plots of soil samples (normalization values from Sun and McDonough 1989). **a** Non-urban soils: filled square: ultramafic derives soils, open square: other samples, **b** HSL, **c** LSS

contributions of  $F_1$ ,  $F_2$ , and  $F_3$  are shown in Fig. 9a. The average contribution was 6.6 and 93.4% for natural and anthropogenic (industrial and leaded petrol) sources, respectively. The contribution of industrial and leaded petrol in the Pb isotope signatures of park soil samples is not so simple. The correlation between Pb content with  $F_2$  (industrial source; Fig. 9b) is generally negative, while this correlation is positive for Pb and  $F_3$  (leaded petrol; Fig. 9c). Detail investigation of Pb isotope and Pb content of park soils (Fig. 9b, c) suggests that industrial source is the main origin of samples with relatively low Pb content (<90 ppm). The contribution of leaded petrol increases in the samples with high Pb. These soils were collected from the central parks of Mashhad which have high traffic intensity.

**Environmental assessment of park soils**

There are some parameters which are used as the index for estimation of soil pollution. The geoaccumulation index ( $I_{geo}$ ) and enrichment factor (EF) were selected to evaluate the soil pollution of Mashhad parks. The geoaccumulation index was calculated by Muller (1969) equation:

$$I_{geo} = \log_2(C_n/1.5 B_n),$$

where  $I_{geo}$  is the geoaccumulation index,  $\log_2$  is log base 2,  $C_n$  is the concentration in the soil, and  $B_n$  is the geochemical background or reference concentration. In this study, the concentration of elements in the earth’s crust (Taylor 1964) was chosen as  $B_n$ . The geoaccumulation index is classified as follows:

$I_{geo} \leq 0$  practically unpolluted environment;  $0 < I_{geo} \leq 1$  unpolluted to moderately polluted;  $1 < I_{geo} \leq 2$  moderately polluted;  $2 < I_{geo} \leq 3$  moderately to strongly polluted;  $3 < I_{geo} \leq 4$  strongly polluted;  $4 < I_{geo} \leq 5$  strongly to extremely polluted; and  $I_{geo} > 5$  extremely polluted.

The enrichment factor (EF) was calculated by following equation (Buat-Menard and Chesselet 1979):

$$EF = C_n/C_{ref}(\text{sample}) = B_n/B_{ref}(\text{background}),$$

where  $C_n$  is the content of the element in the soil,  $C_{ref}$  is the content of the reference element in the soil, and  $B_n$  and  $B_{ref}$  are the concentration of the element and reference elements in the background. Th was chosen as a reference element in this study, because the concentration of this element is similar to crust content and show negligible variation in the studied samples (Supplementary Table 1). Evaluation categories for EF:

EF < 1 indicates no enrichment; EF < 3 minor enrichment; EF = 3–5 moderate enrichment; EF = 5–10 moderately severe enrichment; EF = 10–25 severe enrichment; EF = 25–50 very severe enrichment; EF > 50 extremely severe enrichment.

**Table 2** Pearson correlation coefficient matrix for heavy metals in the park soil samples of Mashhad city

	As	Cd	Co	Cr	Cu	Mn	Mo	Ni	Pb	Se	Sn	Ti	V	Zn
As	1													
Cd	0.35	1												
Co	0.91**	0.57*	1											
Cr	0.94**	0.43	0.96**	1										
Cu	0.67*	0.81**	0.86**	0.77**	1									
Mn	0.84**	0.27	0.82**	0.85**	0.60*	1								
Mo	0.29	0.97**	0.51*	0.37	0.79**	0.19	1							
Ni	0.92**	0.50*	0.95**	0.97**	0.81**	0.83**	0.45	1						
Pb	0.4	0.94**	0.59	0.48	0.84**	0.28	0.96**	0.57*	1					
Se	0.38	0.91**	0.60*	0.48	0.89**	0.28	0.93**	0.57*	0.98**	1				
Sn	0.34	0.97**	0.58*	0.44	0.85**	0.24	0.98**	0.53*	0.91**	0.96**	1			
Ti	0.89**	0.29	0.86**	0.88**	0.58*	0.96**	0.19	0.84**	0.21	0.26	0.24	1		
V	0.83**	0.19	0.80**	0.9**	0.58*	0.94**	0.11	0.85**	0.21	0.23	0.17	0.90**	1	
Zn	0.41	0.99**	0.63*	0.49	0.84**	0.32	0.96**	0.56*	0.94**	0.92**	0.97**	0.35	0.24	1

\*\*Correlation is significant at the 0.01 level (two-tailed)

\*Correlation is significant at the 0.05 level (two-tailed)

The calculated values of EF and  $I_{geo}$  for heavy metals in the soils of Mashhad parks are presented in Tables 3 and 4, respectively. The major part of soil samples shows no enrichment or minor enrichment ( $EF < 3$ ) for Co, Cr, Cu, Ni, and Mo; moderate enrichment of As and Zn; severe enrichment of Pb and Zn (mean  $EF = 12-15$ ); and very severe enrichment of Se (mean  $EF = 47$ ). The geoaccumulation index calculations indicate that there is no sign of heavy metal pollution in the Mashhad park soils, except Pb (mean  $I_{geo} = 2.1$ ) and Sn (mean  $I_{geo} = 2.3$ ) which exhibit moderate-to-strong pollution (Table 4).

The standard limits or maximal permissible concentrations (MPC) for potentially toxic elements of soils differ based on several factors such as regional geology, bedrock lithology, climate, and redox condition and bioavailability (Hooda 2010). Therefore, different countries present distinct standards for environmental programs. The PMC values determined by the Iranian Department of Environment (IDM 2013) and the Canadian Council of Ministers of the Environment (CCME 2007) are included in Supplementary Table 1. The comparison of the soil composition of Mashhad parks with these standards indicates that all elements have lower concentrations than Iranian MPC, while Cr, Cu, Ni, and Se contents in most samples and Pb and Zn concentrations in some samples are higher than CCME limits.

PCA plot in rotated space

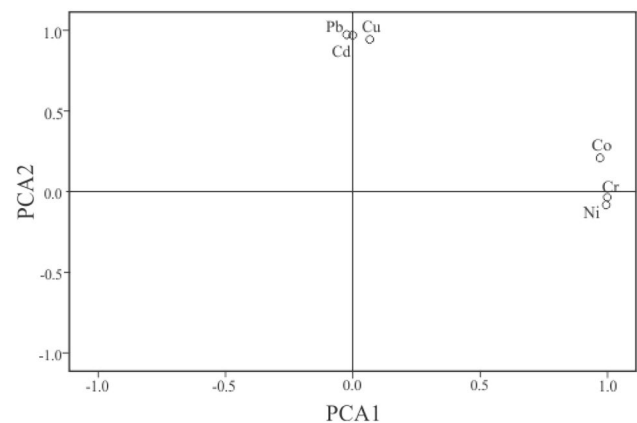
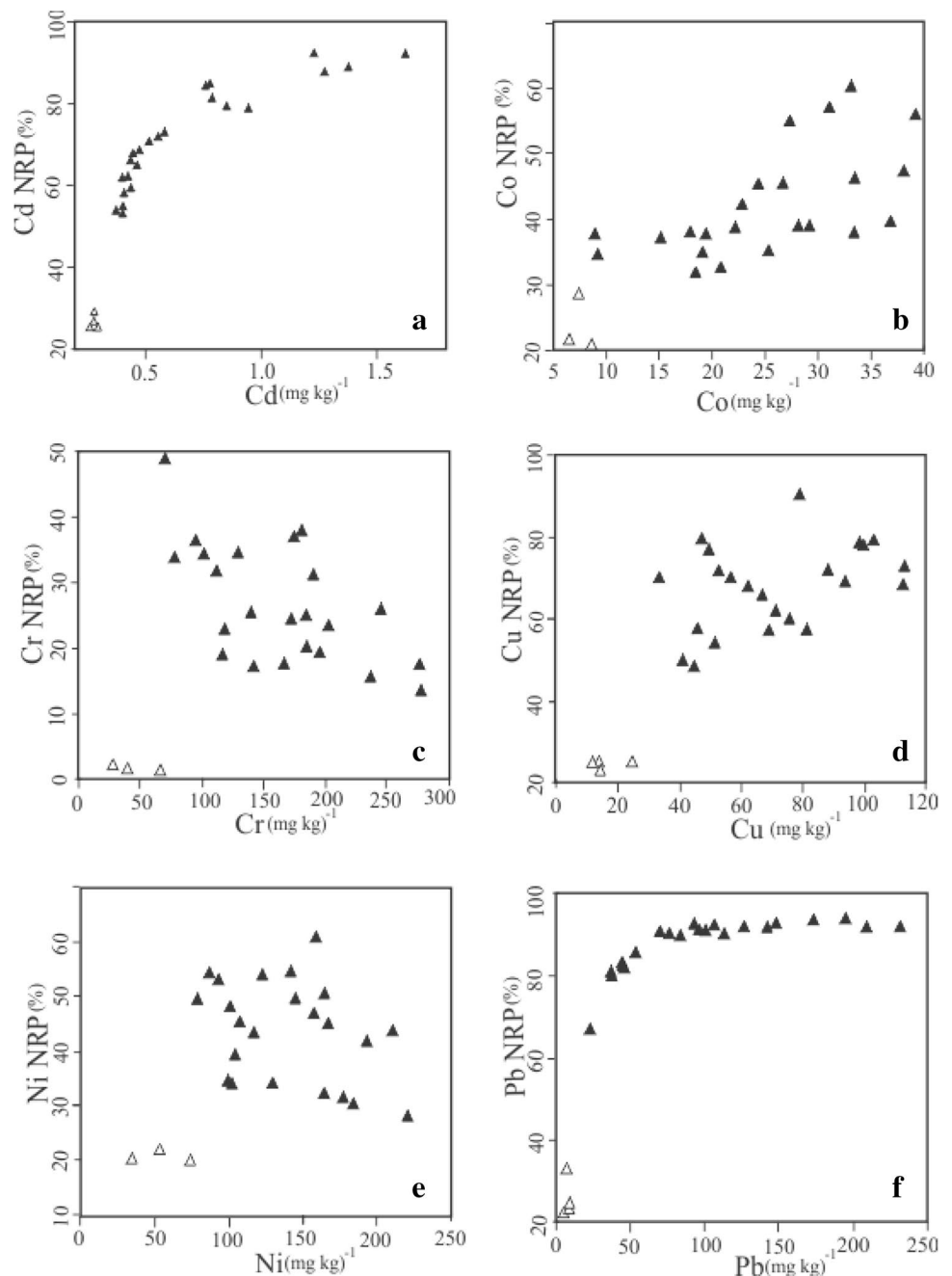


**Fig. 6** PCA diagram of the total concentration of Cd, Co, Cr, Cu, Ni, and Pb in the park soil samples. These two PC components explain 94.49% of total variance. The PC1 and PC2 are accounted for 78.36 and 18.13% of total variance, respectively

## Conclusion

1. The chemical analyses of Mashhad park soils indicate that they could be divided into high silica soils (HSS) and low silica soils (LSS). The HSL group has high concentration of  $SiO_2$  (mean 54 vs. 48 wt% in LSS) and HFSE (high field strength elements), while the LSS samples show high contents of metal elements such as MgO (mean 7 vs. 4 wt% in HSS),  $FeO_t$  (mean 6 vs. 4 wt% in HSS), Co (mean 31 vs. 19  $mg\ kg^{-1}$  in HSS), Cu (mean 83 vs. 57  $mg\ kg^{-1}$  in HSS), Mn (mean 940

**Fig. 7** Binary diagrams display total heavy metal concentrations and non-residual percentage (NRP) of these elements. The ultramafic-derived soil sample (HM-31) is not shown in Co, Cr, and Ni diagrams because of very high concentrations. The symbols are similar to Fig. 2



vs. 370 mg kg<sup>-1</sup> in HSS), Pb (mean 112 vs. 86 mg kg<sup>-1</sup> in HSS), Sn (mean 22 vs. 15 mg kg<sup>-1</sup> in HSS), and Zn (mean 170 vs. 125 mg kg<sup>-1</sup> in HSS). The REE composition of soil samples suggests that the LLS is more similar to ultramafic derived soils and HSS samples are derived from other soils (granitoid, metamorphic and sedimentary derived soils).

2. The concentrations of potentially toxic elements in the park soils of Mashhad city are highly enriched relative to non-urban soils. The PCA results show that the ele-

ments which were originated from natural sources were loaded in PC1. This component exhibits two different positive and negative loadings of metal elements and HFSE, respectively. The anthropogenically derived elements (Cd, Cu, Mo, Pb, Se, Sn, and Zn) were loaded in PC2.

3. The BCR sequential extraction analyses show that park soil samples have higher available heavy metal contents than non-urban soils. The Pb isotope composition of non-urban soils (<sup>206</sup>Pb/<sup>204</sup>Pb = 18.737–19.420 and

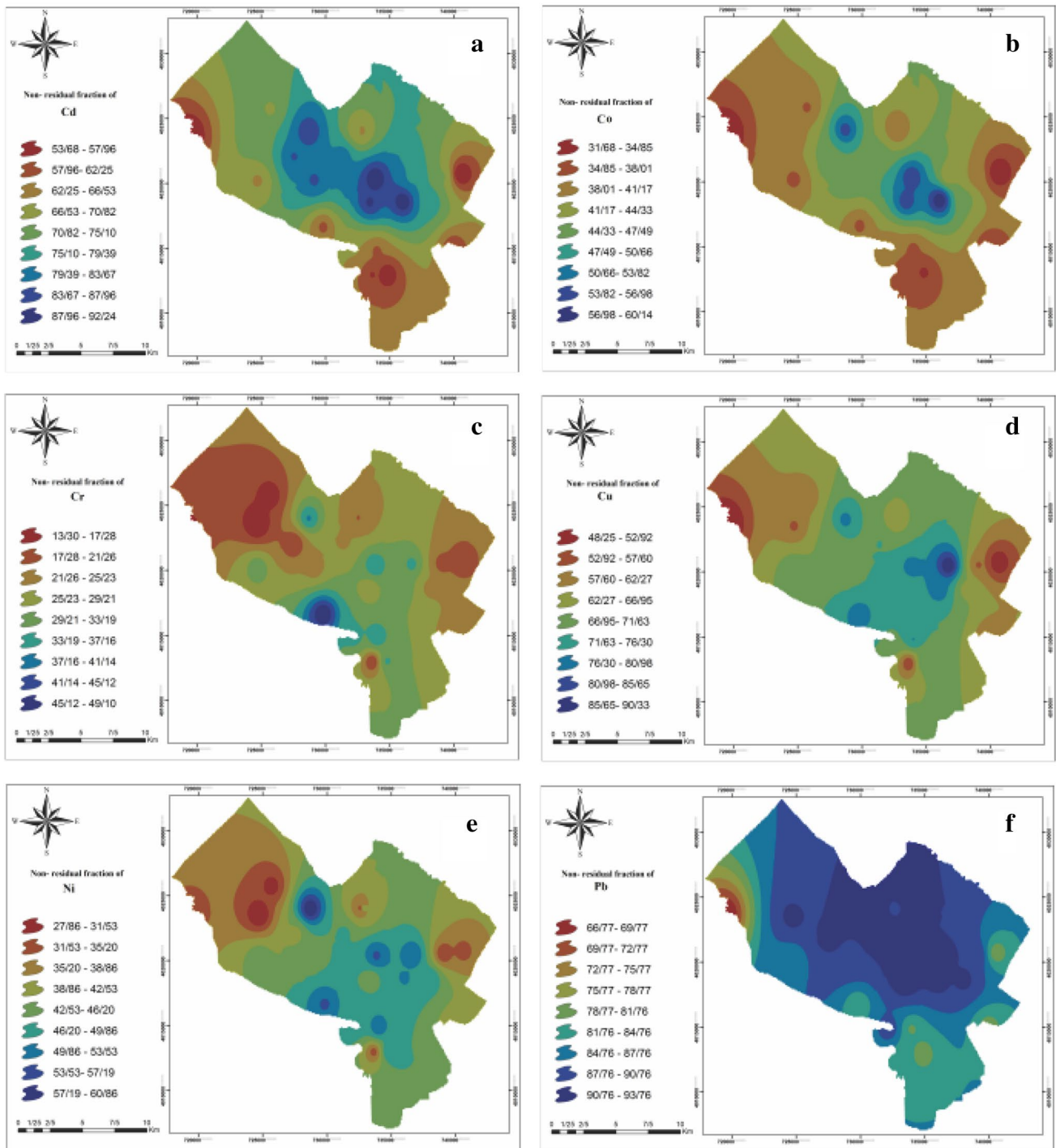
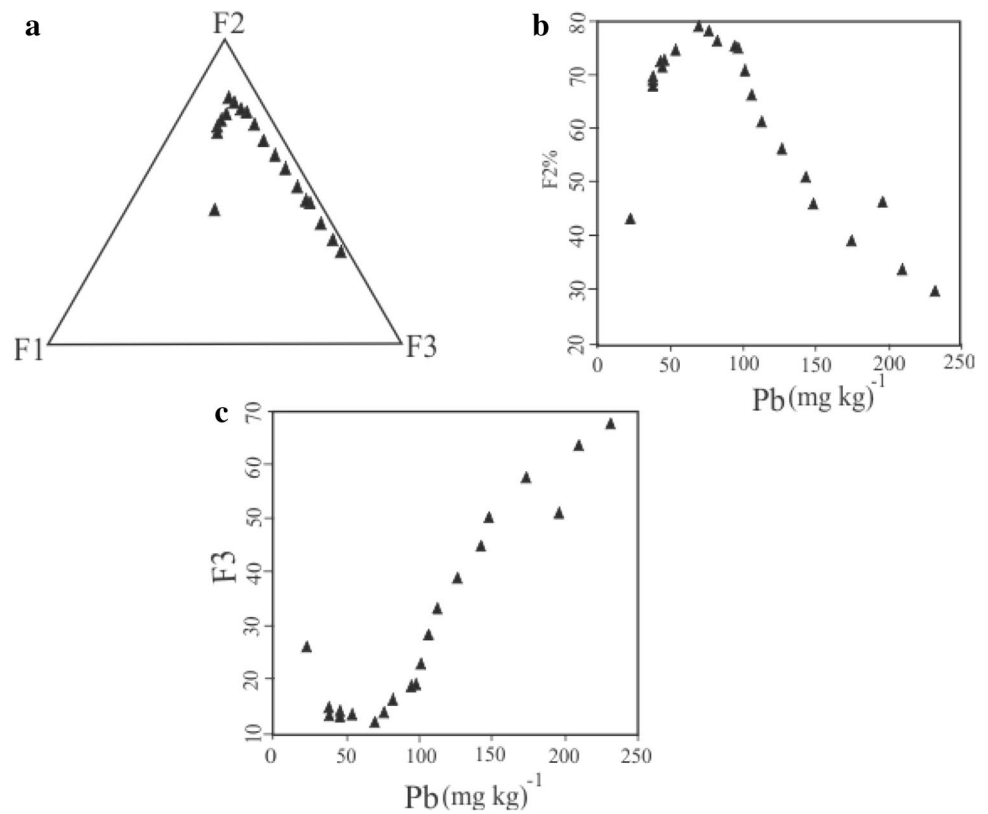


Fig. 8 Spatial distribution of potentially available (non-residual) fractions of Mashhad park soils

**Fig. 9** a Calculated contribution of natural ( $F_1$ ), industrial ( $F_2$ ) and leaded petrol ( $F_3$ ) sources in the soil samples of Mashhad parks. The contribution percentage of industrial (b) and leaded petrol vs. total Pb content (in  $\text{mg kg}^{-1}$ ) of park soil



**Table 3** Calculation of enrichment factors for heavy metals of Mashhad park soils

Sample	EFA <sub>s</sub>	EFC <sub>d</sub>	EFC <sub>o</sub>	EFC <sub>r</sub>	EFC <sub>u</sub>	EF <sub>Ni</sub>	EF <sub>Mo</sub>	EF <sub>Pb</sub>	EF <sub>Se</sub>	EF <sub>Sn</sub>	EF <sub>Zn</sub>
HM-23	3.45	0.57	1.38	2.43	1.70	2.72	2.10	16.09	50.81	17.72	4.09
HM-18	2.42	0.41	1.02	1.45	1.60	1.82	1.61	11.25	26.78	14.46	3.04
HM-9	3.00	0.24	1.00	1.55	1.09	1.84	0.97	4.04	28.92	3.81	1.80
HM-20	1.91	0.18	0.37	0.78	0.61	1.07	0.72	3.13	22.22	3.03	1.21
HM-12	2.70	0.22	0.94	1.48	0.95	1.70	0.92	3.80	58.86	2.43	1.69
HM-21	3.40	0.76	1.52	2.51	2.50	2.94	3.68	25.76	44.51	32.97	4.76
HM-19	2.91	0.25	1.11	1.74	1.40	1.94	1.06	10.09	34.90	10.22	1.84
HM-16	2.47	0.23	0.93	1.33	1.23	1.71	0.97	5.11	35.99	6.66	1.70
HM-2	2.31	0.22	0.83	1.17	1.11	1.55	0.96	7.60	30.06	7.63	1.67
HM-11	2.14	0.18	0.63	0.99	0.93	1.28	0.77	3.82	27.12	3.70	1.29
HM-1	1.85	0.18	0.34	0.68	0.84	1.13	0.77	3.52	35.25	4.21	1.19
HM-15	5.81	0.70	3.25	5.88	4.34	5.49	2.63	18.06	72.51	22.19	5.03
HM-17	4.49	0.56	2.26	3.41	2.86	3.76	2.18	15.13	63.98	19.79	3.96
HM-22	3.75	0.51	1.60	2.76	2.39	3.15	2.36	17.72	32.99	18.45	3.76
HM-6	4.00	0.28	1.61	2.67	1.49	2.76	1.12	5.54	35.19	4.40	2.21
HM-14	3.64	0.25	1.27	2.17	1.23	2.07	1.09	2.71	67.03	2.44	1.90
HM-8	5.22	1.18	3.14	4.90	4.10	5.64	4.80	31.30	83.97	51.60	8.27
HM-4	4.16	1.13	2.15	3.10	3.02	3.58	4.04	27.22	68.32	37.02	7.09
HM-7	3.15	0.71	1.69	2.37	2.42	2.57	2.87	18.80	40.55	28.46	4.54
HM-5	5.33	0.46	2.78	5.24	2.76	5.52	1.59	14.13	52.69	14.31	3.71
HM-13	5.95	0.49	2.99	5.32	3.05	5.47	1.82	13.50	66.96	11.94	3.52
HM-3	4.65	0.35	1.96	3.40	2.24	4.10	1.48	13.46	48.86	11.26	2.64
HM-10	4.04	0.37	1.80	2.85	1.94	3.41	1.28	8.67	48.72	8.90	2.76

**Table 4** Calculation of the geoaccumulation index for heavy metals of Mashhad park soils

Sample	$I_{\text{geo}}\text{As}$	$I_{\text{geo}}\text{Cd}$	$I_{\text{geo}}\text{Co}$	$I_{\text{geo}}\text{Cr}$	$I_{\text{geo}}\text{Cu}$	$I_{\text{geo}}\text{Ni}$	$I_{\text{geo}}\text{Mo}$	$I_{\text{geo}}\text{Pb}$	$I_{\text{geo}}\text{Se}$	$I_{\text{geo}}\text{Sn}$	$I_{\text{geo}}\text{Zn}$
HM-23	0.70	1.65	-0.62	0.20	-0.31	0.36	-0.01	2.93	1.26	3.06	0.95
HM-18	0.53	1.50	-0.72	-0.21	-0.07	0.12	-0.05	2.75	1.26	3.11	0.86
HM-9	0.60	0.52	-0.97	-0.35	-0.86	-0.10	-1.02	1.03	0.68	0.95	-0.13
HM-20	0.33	0.45	-2.03	-0.95	-1.31	-0.51	-1.07	1.05	0.55	1.00	-0.33
HM-12	0.49	0.42	-1.03	-0.37	-1.01	-0.17	-1.06	0.98	0.55	0.34	-0.19
HM-21	0.70	2.08	-0.45	0.27	0.26	0.49	0.82	3.63	1.62	3.98	1.19
HM-19	0.64	0.62	-0.76	-0.10	-0.42	0.05	-0.81	2.43	1.09	2.45	-0.03
HM-16	0.45	0.55	-0.95	-0.43	-0.55	-0.08	-0.89	1.50	0.90	1.89	-0.09
HM-2	0.42	0.58	-1.07	-0.57	-0.65	-0.16	-0.85	2.13	1.00	2.14	-0.05
HM-11	0.45	0.45	-1.31	-0.67	-0.75	-0.29	-1.03	1.29	0.79	1.24	-0.28
HM-1	0.33	0.49	-2.09	-1.10	-0.81	-0.38	-0.93	1.26	0.79	1.52	-0.30
HM-15	0.86	1.34	0.02	0.88	0.44	0.78	-0.28	2.50	1.26	2.79	0.65
HM-17	0.83	1.36	-0.16	0.43	0.18	0.57	-0.21	2.58	1.18	2.97	0.65
HM-22	0.74	1.40	-0.49	0.30	0.09	0.49	0.07	2.98	1.34	3.04	0.74
HM-6	0.74	0.45	-0.57	0.16	-0.69	0.20	-1.10	1.21	0.55	0.87	-0.12
HM-14	0.67	0.34	-0.85	-0.08	-0.90	-0.14	-1.07	0.24	0.55	0.09	-0.26
HM-8	0.80	2.20	0.06	0.71	0.45	0.91	0.68	3.38	1.55	4.10	1.46
HM-4	0.77	2.43	-0.18	0.35	0.31	0.55	0.73	3.48	1.49	3.92	1.54
HM-7	0.64	2.04	-0.27	0.22	0.26	0.34	0.50	3.21	1.49	3.81	1.16
HM-5	0.92	0.93	-0.02	0.89	-0.04	0.97	-0.83	2.32	1.00	2.34	0.40
HM-13	0.83	0.77	-0.16	0.67	-0.14	0.71	-0.88	2.01	0.90	1.83	0.07
HM-3	0.83	0.65	-0.42	0.38	-0.22	0.65	-0.83	2.36	1.00	2.10	0.01
HM-10	0.80	0.90	-0.37	0.30	-0.26	0.55	-0.86	1.90	0.90	1.94	0.25

$^{208}\text{Pb}/^{206}\text{Pb} = 2-2.064$ ) indicates that they have a natural source, while park soil samples ( $^{206}\text{Pb}/^{204}\text{Pb} = 17.284-18.024$  and  $^{208}\text{Pb}/^{206}\text{Pb} = 2.107-2.162$ ) are originated from anthropogenic sources. The soils which sampled from central parks of Mashhad have the highest heavy metal pollution due to high traffic intensity in these areas.

- The concentration of heavy metals in this region is lower than the national standards but the available percentage of these elements is high in the park soils which could be considered in the environmental assessments.

**Funding** Some analytical cost of this project was supported by Payame Noor University. The authors gratefully acknowledge the comments of the anonymous reviewers that helped improve the original manuscript.

## References

- Alavi M (1979) The virani ophiolite complex and surrounding rocks. *Geol Rundsch* 68:334-341
- Alavi M (1991) Sedimentary and structural characteristics of the Paleo-Tethys remnants in northeastern Iran. *Geol Soc Am Bull* 1038:983-992
- Alekseenko V, Alekseenko A (2014) The abundances of chemical elements in urban soils. *J Geochem Explor* 147:245-249
- Alexander EB (2004) Serpentine soil redness, differences among peridotite and serpentinite materials, Klamath Mountains, California. *Int Geol Rev* 46:754-764
- Andersson M, Ottesen RT, Langedal M (2010) Geochemistry of urban surface soils—monitoring in Trondheim, Norway. *Geoderma* 156:112-118
- Argyaki A, Kelepertzis E (2014) Urban soil geochemistry in Athens, Greece: the importance of local geology in controlling the distribution of potentially harmful trace elements. *Sci Total Environ* 482-483:366-377
- Bourliva A, Papadopoulou L, Aidona E, Giouri K (2017) Magnetic signature, geochemistry, and oral bioaccessibility of technogenic metals in contaminated industrial soils from Sindos Industrial Area, Northern Greece. *Environ Sci Pollut Res* 24:17041-17055
- Buat-Menard P, Chesselet R (1979) Variable influence of the atmospheric flux on the trace metal chemistry of oceanic suspended matter. *Earth Planet Sci Lett* 42:398-411
- CCME (Canadian Council of Ministers of the Environment) (2007) Canadian soil quality guidelines for the protection of environmental and human health: summary tables. Canadian environmental quality guidelines. <http://ceqg-rcqe.ccme.ca/download/en/342/>
- EPMC (Environmental Pollution Control of Mashhad) (2017) 2016 air quality report of Mashhad (in Persian)
- Ferri R, Donna F, Smith DR, Guazzetti S, Zacco A, Rizzo L, Bontempi E, Zimmerman NJ, Lucchini RG (2012) Heavy metals in soil and salad in the proximity of historical ferroalloy emission. *J Environ Prot* 3:374-385
- Frostick A, Bollhöfer A, Parry D, Munksgaard N, Evans K (2008) Radioactive and radiogenic isotopes in sediments from Cooper Creek, Western Arnhem land. *J Environ Radioact* 99:468-482
- Galušková I, Mihaljevič M, Borůvka L, Drábek O, Frühauf M, Němeček K (2014) Lead isotope composition and risk elements



- distribution in urban soils of historically different cities Ostrava and Prague, the Czech Republic. *J Geochem Explor* 147:215–221
- Giusti L (2013) The chemistry and parent material of urban soils in Bristol (UK): implications for contaminated land assessment. *Environ Geochem Health* 35:53–67
- Gu YG, Gao YP, Lin Q (2016) Contamination, bioaccessibility and human health risk of heavy metals in exposed-lawn soils from 28 urban parks in southern China's largest city, Guangzhou. *Appl Geochem* 67:52–58
- Hansmann W, Köppel V (2000) Lead-isotopes as tracers of pollutants in soils. *Chem Geol* 171:123–144
- Hooda PS (2010) Trace elements in soils. Wiley, New York
- Horvath A, Szita R, Bidlo A, Gribovszki Z (2016) Changes in soil and sediment properties due the impact of the urban environment. *Environ Earth Sci* 75:1211. <https://doi.org/10.1007/s12665-016-6012-8>
- IDM (Iranian Department of Science) (2013) The standards of soil quality and guidelines (in Persian)
- Jin L, Ma L, Dere A, White T, Mathur R, Brantley SL (2017) REE mobility and fractionation during shale weathering along a climate gradient. *Chem Geol* 466:352–379
- Karimi A, Haghnia GH, Safari T, Hadadian H (2017) Lithogenic and anthropogenic pollution assessment of Ni, Zn and Pb in surface soils of Mashhad plain, northeastern Iran. *Catena* 157:151–162
- Kelepertzis E, Argyraki A (2015) Geochemical associations for evaluating the availability of potentially harmful elements in urban soils: lessons learnt from Athens, Greece. *Appl Geochem* 512–513:94–102
- Komárek M, Ettler V, Chrastny V, Mihaljevic M (2008) Lead isotopes in environmental sciences: a review. *Environ Int* 34:562–577
- Li H, Yu S, Li G, Deng H, Luo X (2011) Contamination and source differentiation of Pb in park soils along an urban–rural gradient in Shanghai. *Environ Pollut* 159:3536–3344
- Liu Z, Pan S, Sun Z, Ma F, Chen L, Wang Y, Wang S (2015) Heavy metal spatial variability and historical changes in the Yangtze River estuary and North Jiangsu tidal flat. *Mar Pollut Bull* 98:115–129
- Loska K, Wiechuya D (2003) Application of principle component analysis for the estimation of source of heavy metal contamination in surface sediments from the Rybnik Reservoir. *Chemosphere* 51:723–733
- Mazhari SA, Sharifiyan Attar R (2015) Rare earth elements in surface soils of the Davarzan area, NE of Iran. *Geod Reg* 5:25–33
- Mazhari SA, Mazloumi Bajestani AR, Sharifiyan Attar R (2013) Geochemical investigation of Davarzan surface soils, west of Sabzevar, NE Iran. *Iran J Earth Sci* 5:43–53
- Mazhari SA, Sharifiyan Attar R, Haghghi F (2017) Heavy metals concentration and availability of different soils in Sabzevar area, NE of Iran. *J Afr Earth Sci* 134:106–112
- Mirnejad H, Lalonde AE, Obeid M, Hassanzadeh J (2013) Geochemistry and petrogenesis of Mashhad granitoids: an insight into the geodynamic history of the Paleo-Tethys in northeast of Iran. *Lithos* 170–171:105–116
- Monna F, Aiuppa A, Varrica D, Dongarra G (1999) Pb isotope composition in lichens and aerosols from eastern Sicily: insights into the regional impact of volcanoes on the environment. *Environ Sci Technol* 33:2517–2523
- Morel JL, Charzyn'ski P, Shaw RK, Zhang G (2015) The seventh SUITMA conference held in Toruń, Poland. *J Soils Sediments* 15:1657–1658
- Muller G (1969) Index of geo-accumulation in sediments of the Rhine river. *Geojournal* 2:108–118
- Nabavi MH (1976) Introduction to geology of Iran. Geological Survey of Iran Press, Tehran (in Persian)
- Rauret G, Lopez-Sanchez JF, Sahuquillo A, Barahona E, Lachica M, Ure AM, Davidson CM, Gomez A, Luck D, Bacon J, Yli-Halla M, Muntaub H, Quevauvillieri P (2000) Application of a modified BCR sequential extraction (three-step) procedure for the determination of extractable trace metal contents in a sewage sludge amended soil reference material (CRM 483) complemented by a three-year stability study of acetic acid and EDTA extractable metal content. *J Environ Monit* 2:228–233
- Reid MK, Spencer KL (2009) Use of principal components analysis (PCA) on estuarine sediment datasets: the effect of data pre-treatment. *Environ Pollut* 157:2275–2281
- Rodríguez L, Ruiz E, Alonso-Azcárate J, Rincón J (2009) Heavy metal distribution and chemical speciation in tailings and soils around a Pb–Zn mine in Spain. *J Environ Manage* 90:1106–1116
- Rodríguez-Seijo A, Arenas-Lago D, Andrade ML, Vega FA (2015) Identifying sources of Pb pollution in urban soils by means of MC-ICP-MS and TOF-SIMS. *Environ Sci Pollut Res* 22:7859–7872
- Rollinson HR (1993) Using geochemical data: evaluation, presentation, interpretation. Longman Scientific & Technical, London
- Schilling J, Reimann C, Roberts D (2014) REE potential of the Nordkinn Peninsula, North Norway: a comparison of soil and bedrock composition. *Appl Geochem* 41:95–106
- Sun SS, McDonough WF (1989) Chemical and isotopic systematics of the oceanic basalts: implications for mantle composition and processes. In: Saunders AD, Norry MJ (eds) *Magmatism in the Oceanic Basalts*. Geol Soc London, London, pp 313–345
- Taheri J, Ghaemi F (1994) The 1:100000 quadrangle geological map of Mashhad. Geological Survey of Iran, Tehran
- Taylor SR (1964) Abundance of chemical elements in the continental crust: a new table. *Geochim Cosmochim Acta* 28:1273–1285
- Ure AM, Davidson CM (1995) Chemical speciation in the environment. Blackie, Glasgow
- Yang Z, Lu W, Long Y, Bao X, Yang Q (2011) Assessment of heavy metals contamination in urban topsoil from Changchun City, China. *J Geochem Explor* 108:27–38
- Yang J, Meng XZ, Duan YP, Liu LZ, Chen L, Cheng H (2014) Spatial distributions and sources of heavy metals in sediment from public park in Shanghai, the Yangtze River Delta. *Appl Geochem* 44:54–60